Pattern Recognition Coursework
Maria Stamatopoulou ms2520 CID:01977521 Michal Olak mro20 CID: 01985975

Data Preparation

Data The data for all objects from each variable were plotted for all trials. Figure: A1.0 a-b, depicts the plots for trials 5 and 9. There was no significant difference between trials, however trail 9 displays a slightly bigger distinction between objects, hence it will be used for the following analysis. For more clarity Figure: A1.1 a-d, depicts the individual figures for each variable. It is observed that it is harder to differentiate between objects in the case of Vibration (Figure: A1.1 a). The time array is chosen to be 100ms as used in the reference paper. The instance of interest is the 480th instance, or 48s as it occurs during the hold phase of the experiment. During the Hold phase, the robot holds the object for ten seconds and it achieves thermal equilibrium, giving a more stable data pattern and best object differentiation. Vibration data shows object distinction for a very small time interval at the beginning, which does not coincide with other sensor data patterns. Pressure, Temperature and Electrode data provide overall stable patterns for all objects and good distinction between them, for the given time instance. Examining Figure: A1.2 it can be further seen that there is data repetition every 3 ms, corresponding to 30 samples with no new information. Hence 3s will be the chosen time step. For the 9th trial it was easier to decide on a single instance as the objects appeared more distinctable and the data was more stable. This does not occur in the case of the 5th or other trials (refer to Figure: A1.0), where maximum object distinction for the different variables occur in different time intervals. This would not allow object differentiation and would make data analysis harder down the pipeline.

Sampled Data Sampling the data for the mentioned time instance, resulted in the Figures A1.3 and A1.4 that can be found in the appendix. Figure A1.3 displays the PVT data, Figure A1.4a the sampled data for electrode 11 and Figure A1.4b the sampled data from all 19 electrodes. Finger F0 was chosen as there was no significant difference between finger data.

3D Data The 3D representation of the sampled PVT data is depicted in Figure: A1.4 in the Appendix. The different colours represent the different objects. There are 10 points per object, corresponding to one of the 10 trials.

Principal Component Analysis (PCA)

Pressure, Vibration, Temperature (PVT) In order to apply PCA, the PVT data was firstly standardized to zero mean and standard deviation of 1. Next, the covariances between features were calculated and concatenated into covariance matrix. Finally, the eigenvectors and eigenvalues of the covariance matrix were calculated giving respectively the principal components and their variances. The results can be found in Table 1. The standardised data was plotted

PVT PCA	Values(mm)
Covariance Matrix	$\begin{bmatrix} 1.000 & -0.375 & -0.308 \\ -0.375 & 1.000 & 0.165 \\ -0.308 & 0.165 & 1.000 \end{bmatrix}$
Eigenvectors	$\begin{bmatrix} 0.701 & 0.028 & 0.713 \\ -0.320 & 0.906 & 0.279 \\ -0.638 & -0.423 & 0.644 \end{bmatrix}$
Eigenvalues	[1.558 0.982 0.461]

Table 1. T1.2 Results of PCA on PVT data

with added vectors representing the principal components as shown in Figure B1.1. The PCA technique allows for dimensionality reduction with limited loss of information. Reduction to two dimensions using the two principal components with the highest variance was illustrated in Figure B1.2.

Looking at the three principal components (PC) plotted in Figure B1.3 it can be seen that their distributions of data differ significantly. The first PC is characterised by noticeably larger variance of data when compared to the second one and significantly larger when compared to the third one. It implies that the first component may encode more information through higher variance and thus the amount of information carried by each component decreases. This creates favourable conditions for dimensionality reduction by discarding the last one or two PCs.

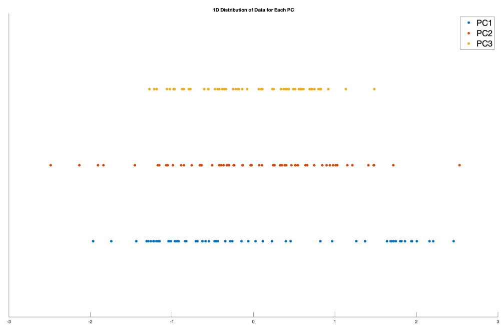

Figure 1. PVT data distribution across Principal Components

Electrodes A haptic sensor consists of 19 electrodes, which hinders effective working with data - both in terms of visualisation and pattern recognition. PCA can be applied to the electrodes data in order to gain insights about underlying data distribution.

The procedure outlined in the PVT PCA section was applied to the electrode data. The obtained principal components were sorted by their eignevalues and the result was illustrated as Scree plot visible in Figure B1.4. It can be seen that the first principal component is characterised by much greater variance than any other. The second component has half the variance and then the value decreases rapidly to almost negligible values after the third component. Thus, it can be assumed that the first three principal components carry most of the electrodes' information. Their values were plotted against each other, presented in Figure B1.5.

Overall it can be concluded that PCA allows for a significant dimensionality reduction of the electrodes data. The first three principal components have significantly more variance in their data distribution then the following sixteen components, which can be consequently discarded without the scarification of a sizeable amount of information.

Linear Discriminant Analysis (LDA)

Black Foam and Car Sponge The results of two dimensional analysis are displayed in Figure C1.1 a-c. The results of three dimensional analysis are displayed in Figure C1.2 a-c.

Black foam and Car sponge objects have relatively similar texture and both belong to the foam object category, rendering relatively challenging to differentiate. When sampling the data from the sensors, the values of these objects were relatively close, especially for vibration sensor data, and followed a similar pattern through time (Figure A1.3a-d). Examining Figure C2.1 a-c it can be observed that LDA succeeded in separating the objects to a certain extent. In the case of Pressure vs Vibration, object means are relatively close and the data is not greatly concentrated around the means. In the Pressure vs Temperature instance, objects means are still close to each other, however the data points are better separated and more concentrated around the corresponding means. Examining Vibration vs Temperature, the object means are largely separated but there is a great overlap between the objects. LDA was the most successful for the instance of Pressure vs Temperature, which was to be expected as it is the only case that does not involve Vibrational data. Performing LDA in the complete dataset led to the better separation of the objects (Figure C1.2 a-c).

Acrylic and Car Sponge The acrylic and car sponge were chosen for additional analysis as they have very different physical properties. There was a clear distinction between the objects for all sensors (Figure A1.3a-d), therefore it is expected that the LDA algorithm should successfully separate the two objects, while keeping within object data concentrated. After performing the LDA the aforementioned prediction was verified, as the objects were successfully separated. This is displayed in Appendix Figure C2.1 a-c and Figure C2.2 a-c. From Figure C2.1 a-c it can be observed that LDA was successful in separating the objects for all sensors. In the case of Vibration vs Temperature there is an overlap of the object data, which could be a result of data overlap in the Vibration sensor data as displayed in Figure A1.3a. As Displayed in Figure C2.2 a-b, LDA was more successful for objects of different physical properties.

Clustering

Eucledian K-means Clustering The results are displayed in Appendix, Figure D1.2

Overall the clustering performed well. It was successful in separating the data into 6 clusters of equal size. To evaluate the accuracy we compare the clustering output (Figure D1.2) to the original data visualisation with plotted means of every object (Figure D1.1). Overall, the clustering resembles a lot the original data and the centroids correspond to the means very closely. It was successful in separating the flour sack and kitchen objects, even though their data appears to overlap and if we look back at the sampling data, Figure A.1.3, the two objects are closest to each other in all sensor values. Clustering only failed to properly separate the data for clusters 2 and 3, which corresponded to the steal vase and acrylic objects respectively. The above could be attributed to the fact that the data for those objects is the most dispersed from the mean, when compared to the other ones.

City block K-means Clustering The results are displayed in Appendix,Figure: D1.3.

K-means clustering using City block was less successful than Euclidean. It succeeded in detecting the class for the black foam and car sponge objects, as well as the acrylic and steal vase objects, but failed to correctly recognise the kitchen sponge object. The above could be a result of the data being very dispersed, making it harder to cluster. The centroids appeared further from the true means than in the case of the Euclidean distance metric. Both algorithms detected a cluster at the center of the 3D plot that does not correspond to an existing object. This could be attributed to the dispersed, overlapping data points, rendering it challenging to correctly identify the acrylic and kitchen sponge clusters. The overlap of the data could be a result of objects overlap in the vibration sensor data.

Clustering of Electrodes data The same Euclidean and City block clustering methods were applied to the three dimensional electrodes data. The three dimensions represented by the three principal components with the highest variance. The results of this can be seen in Figures D2.1,D2.2, D2.3.

Bagging of Electrodes data An approach alternative to the unsupervised K-means is a supervised machine learning technique Bagging, standing for Bootstrap Aggregation. It was applied in series with decision trees, together creating Random Forest approach.

The data was first randomly split 60/40 into training and validation sets. Then, the training set was fed into MATLAB TreeBagger function with the trees count of 50. The trained model was used to predict labels on the training data. A visualisation of two decision tree is displayed in Figure D2.5 a-b.

The outcome of bagging and classification is visualised as Confusion Matrix between the real and predicted labels presented in Figure D2.4. It indicated that the algorithm has objectively high accuracy with only steel vase and acrylic points being misclassified. It was found that increasing the tree count did not increase the classifier accuracy.

Conclusions

Pattern recognition and data analysis Patter recognition helped to gain insights into the data and effectively allowed to establish how different objects differentiate between each other. It therefore enabled for objects classification based on their physical properties. PCA allowed for dimensionality reduction without significant information loss by finding the directions of greatest data variance. This in turn helped with electrodes data clustering and bagging and further visualisation. LDA gave insights about which objects could be easily separated based on their physical properties. It was found that some objects such as acrylic and car sponge could be accurately distinguished, whereas data from more similar objects such us Black foam and car sponge cannot be separated or concentrated around the mean easily. Clustering provided an overall satisfactory object detection.

Haptics-based classification Overall, object distinction was more successful for objects of different physical properties (eg Acrylic and Car Sponge). If the objects belonged to the same material category (Car sponge and Black Foam), distinguishing between them was more challenging. However, clustering and bagging of the sensor data allowed overall distinction of all objects, hence it can be concluded that haptic feedback is, to a reasonable extent, successful in objects classification. The objects that were repeatedly unsuccessfully classified were the Acrylic and Steel Vase. This could be justified when looking back at the sampled data and recognising that these objects were the least separated among all of the pairs for all sensor data. Both materials were characterised by similar strength and stiffness, which differentiate them from softer porous materials but made it harder to differentiate between themselves.

Sensor redundancy The vibration sensor did not provide information useful for object distinction due to large overlap between the objects. The above could be verified when observing object distinction in 2D data visualisation with and without Vibration data (Figure E1.1). This affected LDA results, where plots involving vibration resulted in the least accurate separability of the data. Thus, sensing of the vibration data could be disregarded as it does not provide insightful information. The Pressure, Temperature and Electrode provided insightful data for object separation. Temperature data has provided stable object patterns, as the objects reached a constant temperature in the hold phase. Analogical behavior was observed in the electrodes data. Therefore, it would be possible to achieve similar overall results with fewer sensing modalities.

Alternative data preparation An alternative method for data sampling would be to calculate the mean values for each object from each sensor over a whole hold phase as opposed to a single point. This would allow an indication of the average trend of the data, as well as reduce it to lower dimension, allowing performance of patter recognition algorithms. In contrast to a time instance, the mean also provides information gained from all the data points within the object-sensor pair, making between object comparison more targeted. However, the mean is affected by noise and might not be representative of the actual average behavior of the object. Also, maximum object distinction and mean position of each object might not coincide, making data separation harder and thus rendering harder for patter recognition algorithms to distinguish between objects.

Appendix

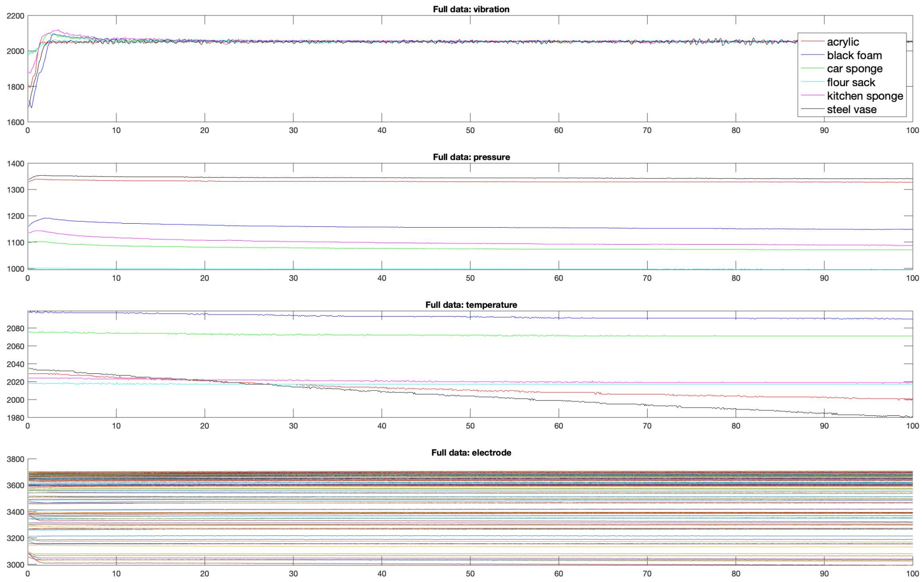

(a) Trial =5

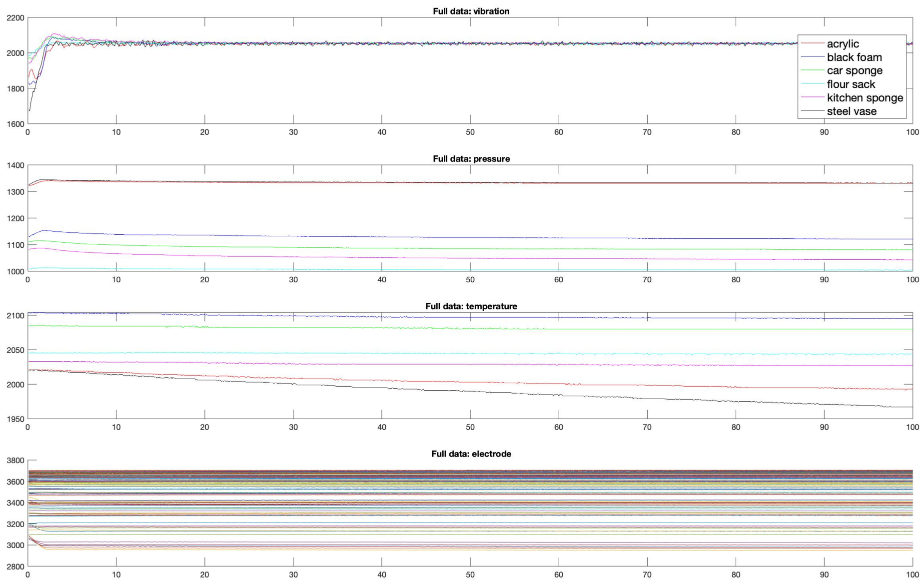

(b) Trial =9

Figure A1.0: Full Data For Trails 5,9 (Measured in ms)

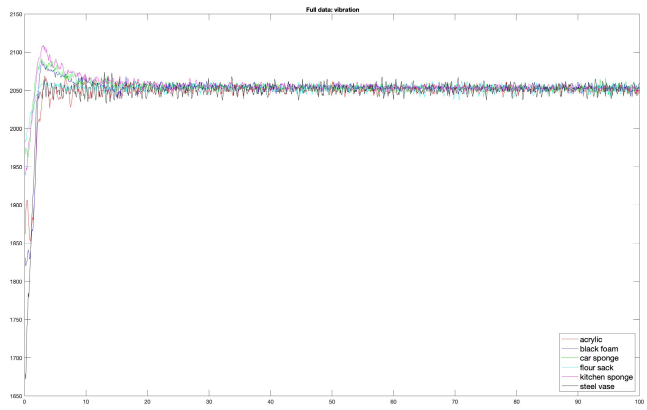

(a) Vibration Data

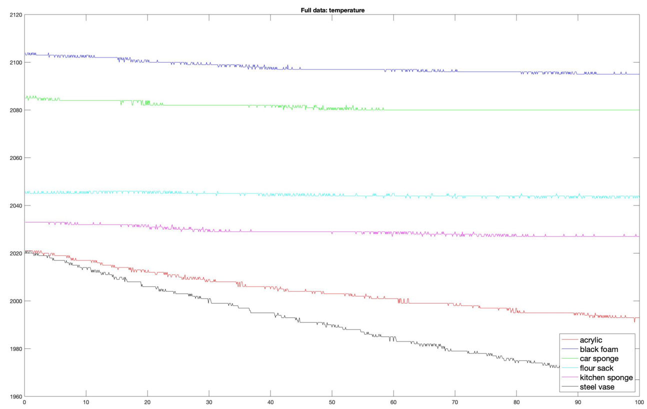

(b) Pressure Data

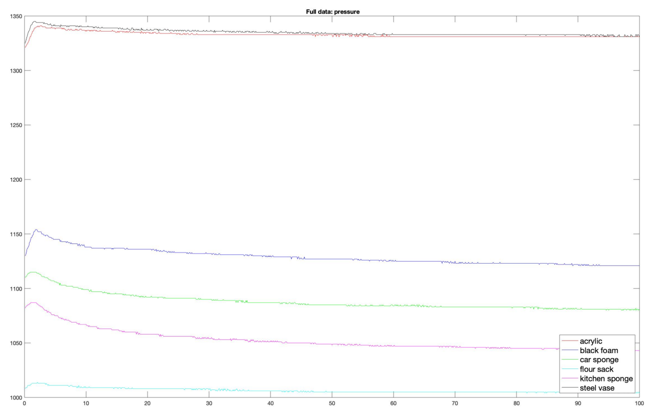

(c) Temperature Data

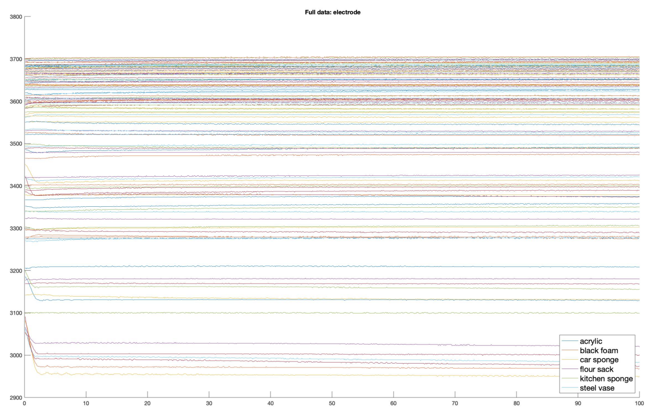

(d) Electrode Data

Figure A1.1: Full Data for Trial =9, (Measured in ms)

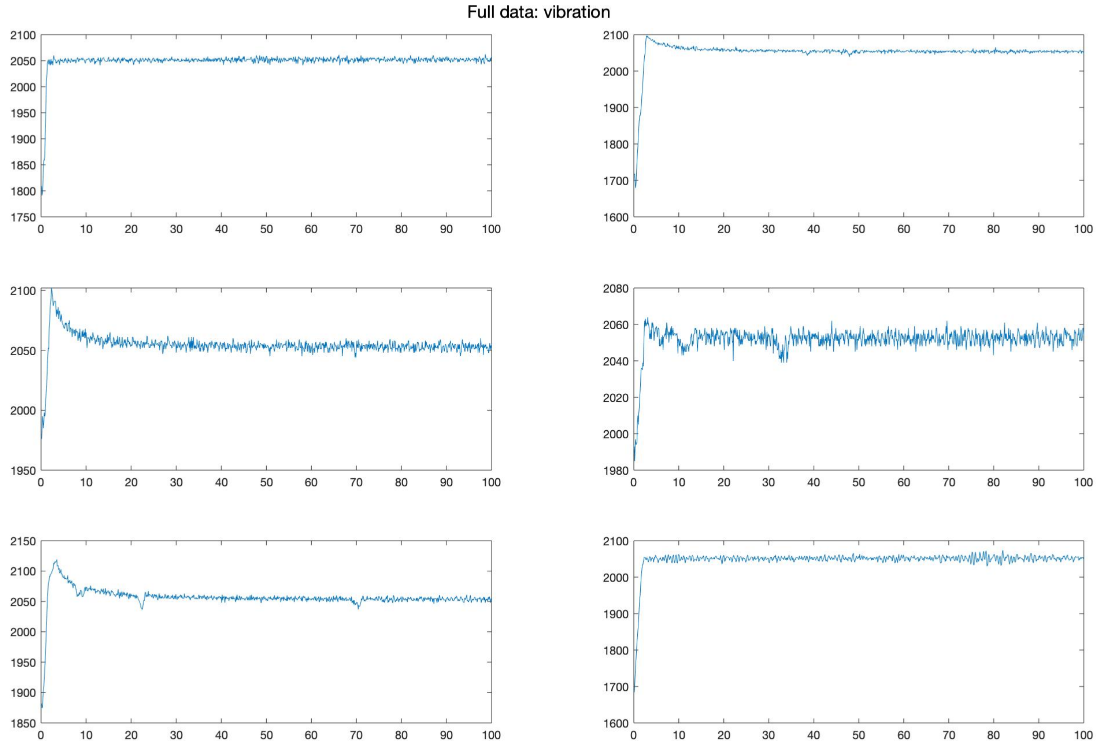

Figure A1.2: Vibration Data for Trial =9: Separate Objects (From top right: Acrylic, Black Foam, car Sponge,Flour Sack, Kitchen Sponge, Steel Vase),(Measured in ms)

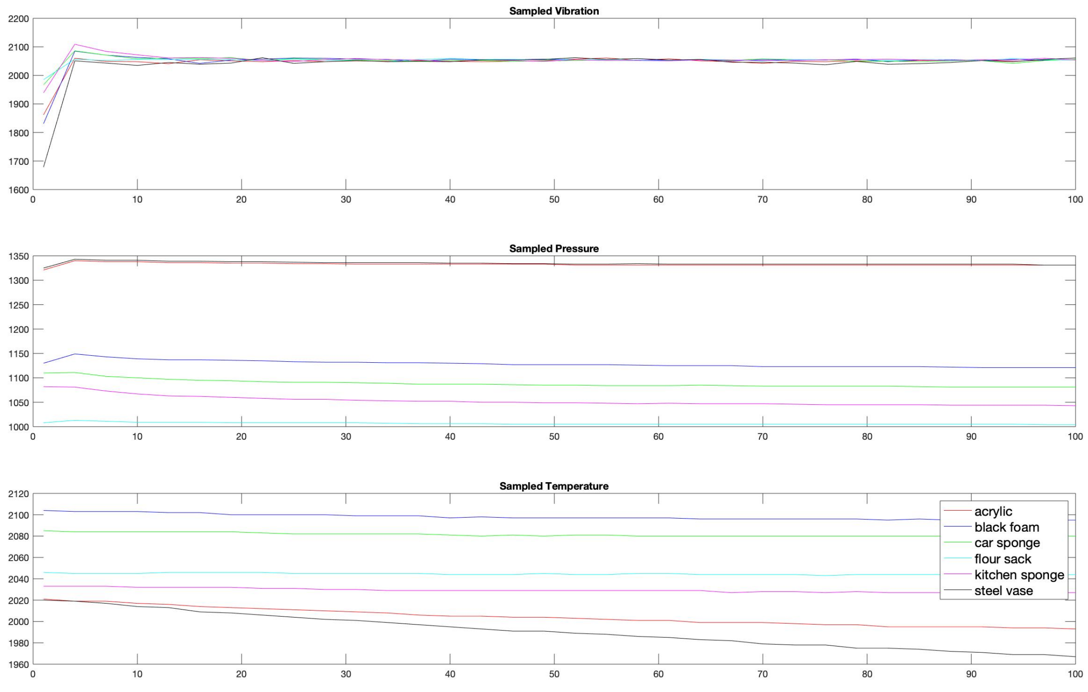

Figure 3: A1.3: PVT Sampled Data, (Measured in ms)

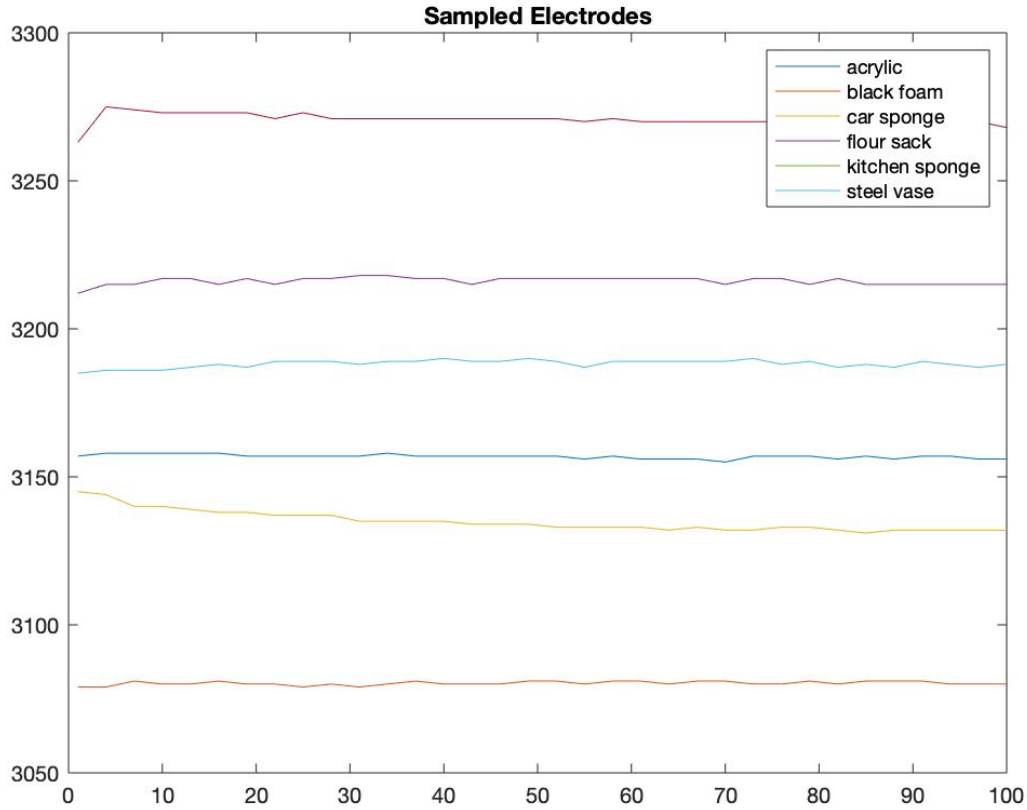

(a) b. Electrode Sampled Data for Electrode 11

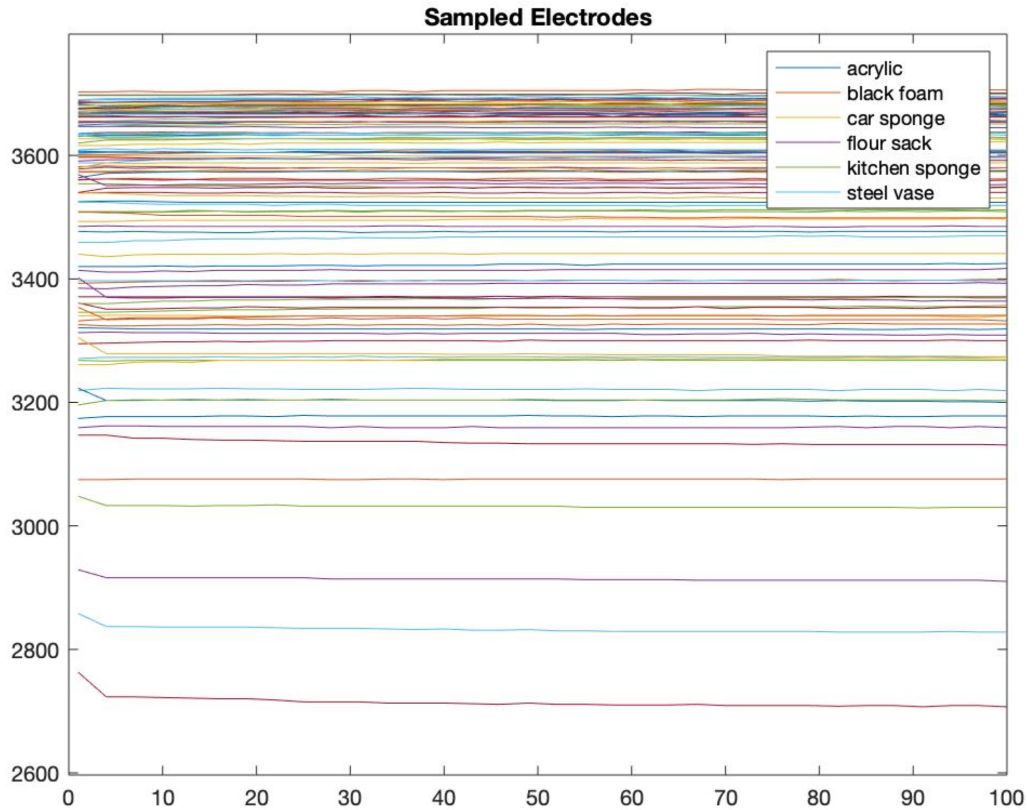

(b) c. Electrode Sampled Data for All Electrodes

Figure A1.4: Sampled Data for Time instance = 48ms, (Measured in ms)

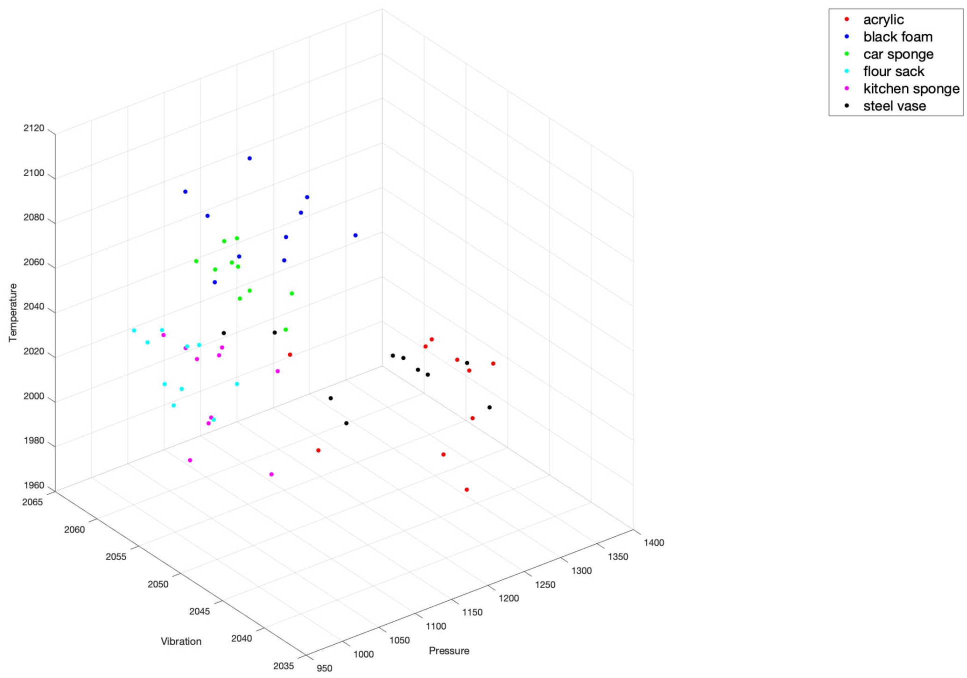

Figure A1.4: 3D Represntation of Sampled Data for Trial =9)

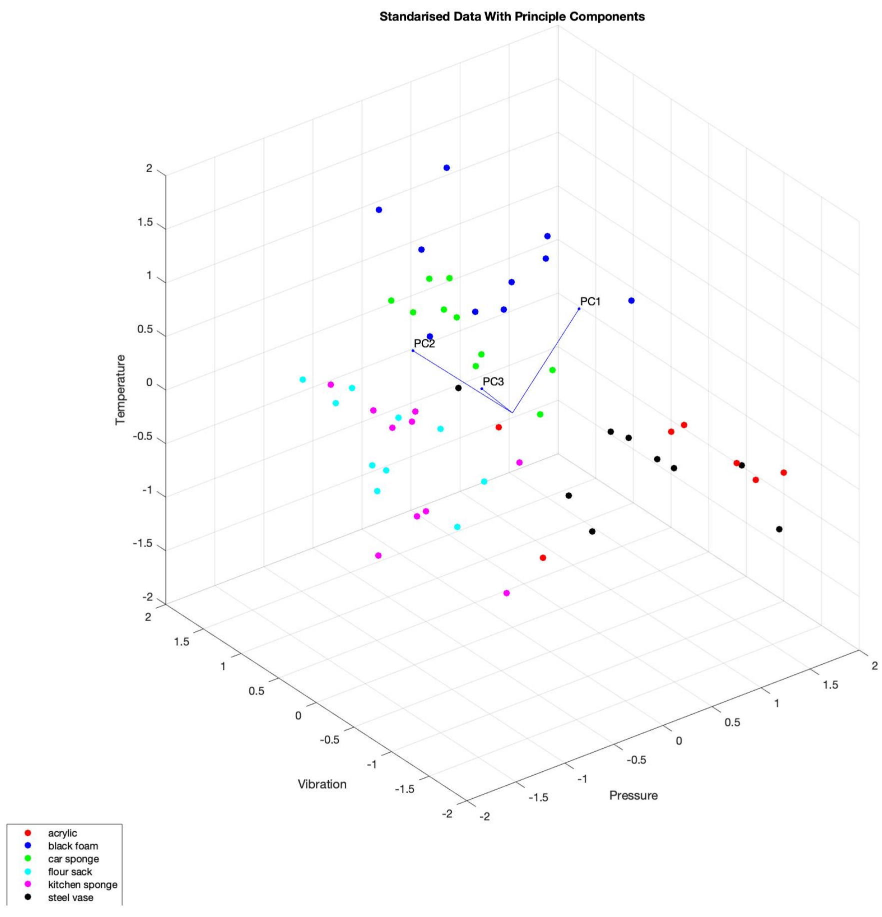

Figure B1.1: 3D Standarised Data With Principle Components

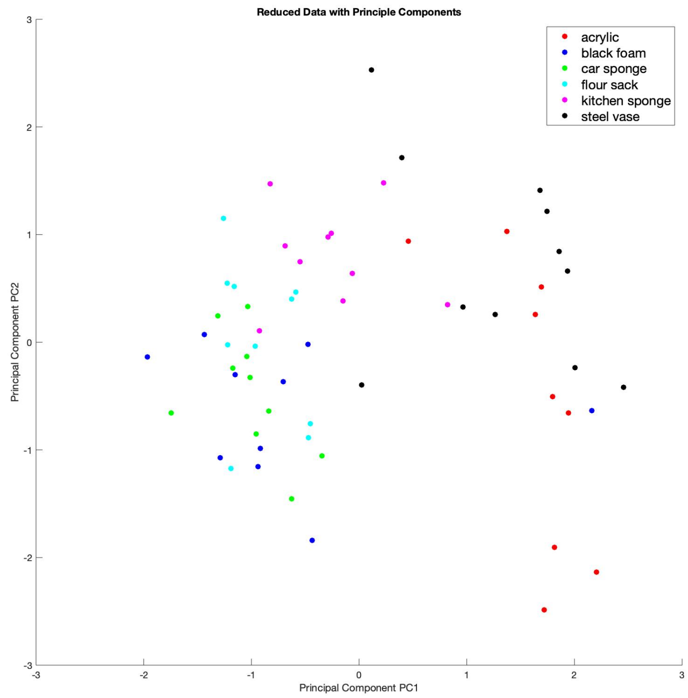

Figure B1.2: 2D Data with Principle Components

Figure B1.3: 1D Principle Components

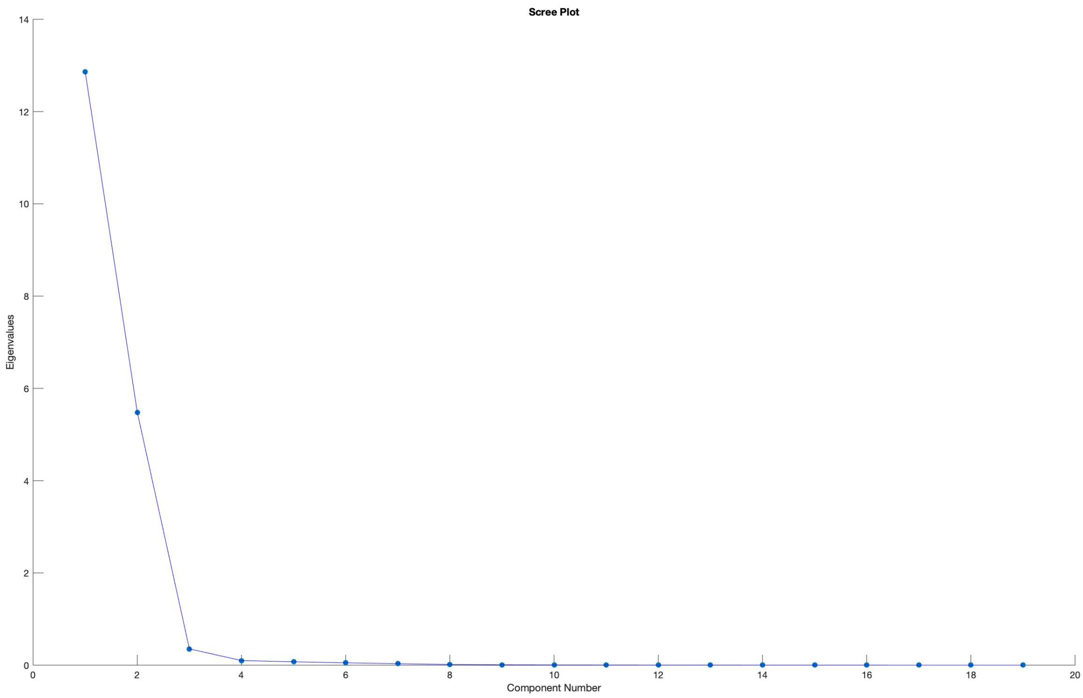

Figure B1.4: Electrode Data Scree Plot

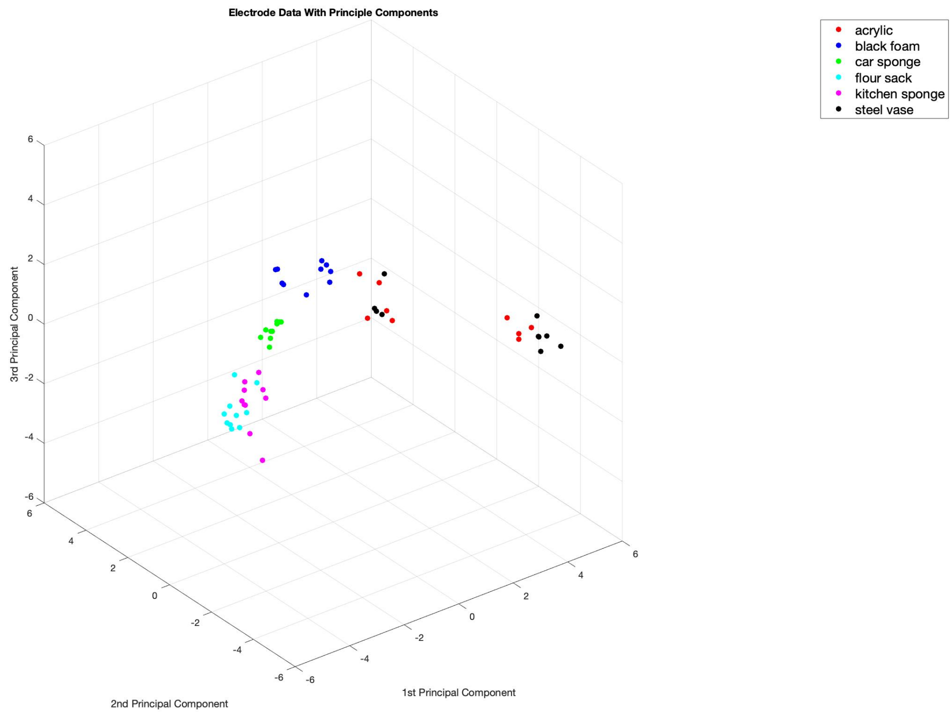

Figure B1.5: Electrode Data- 3 Principle Components

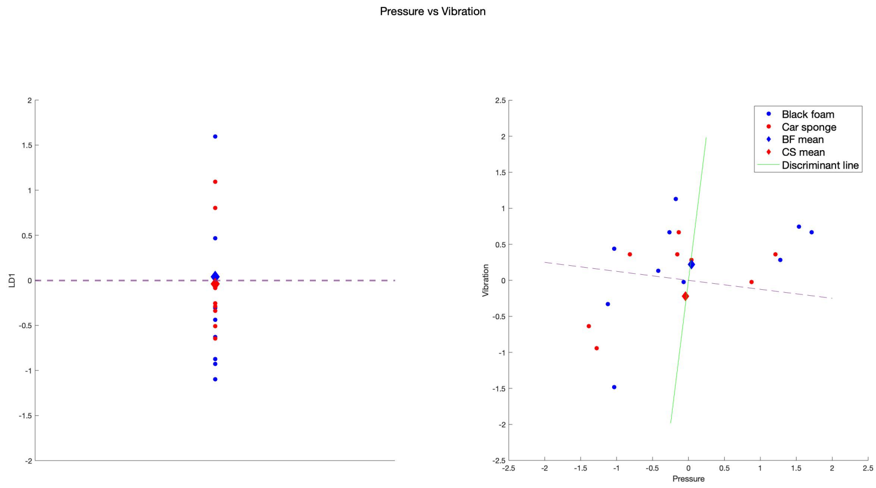

(a) Pressure vs Vibration

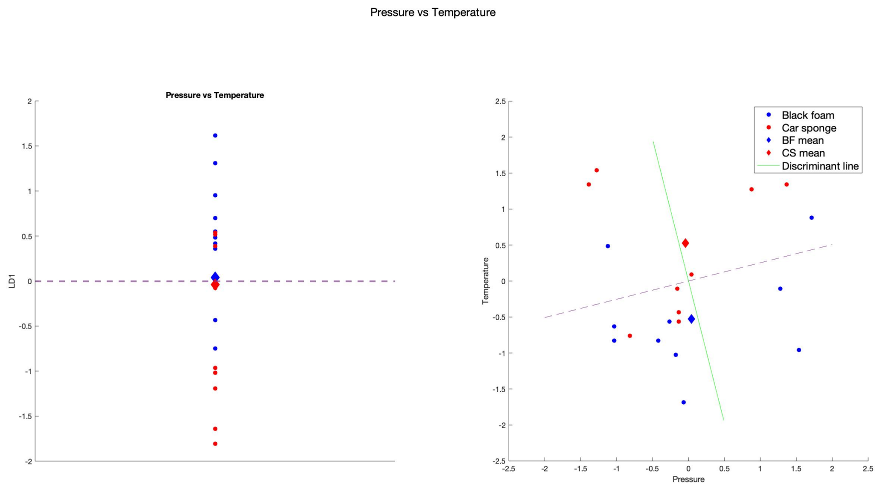

(b) Pressure vs Temperature

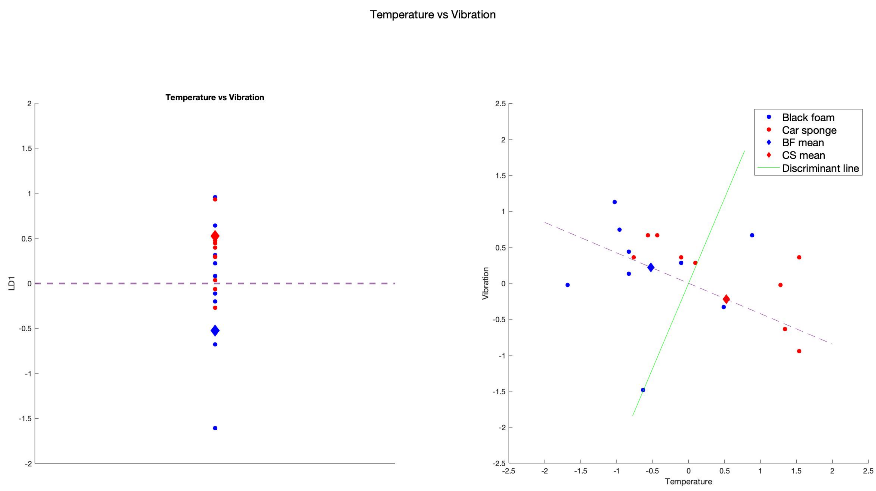

(c) Vibration vs Temperature

Figure C1.1: LDA Data for Black Foam and Car Sponge Objects

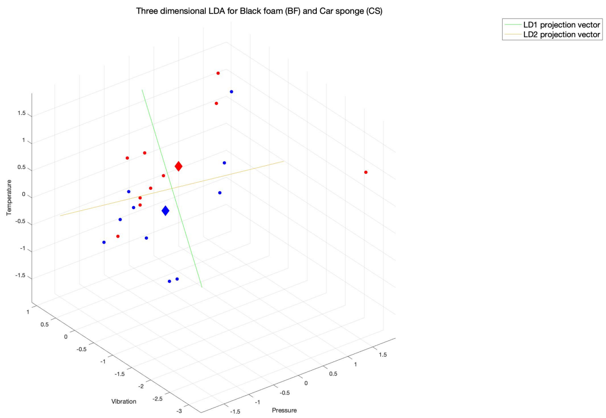

(a) 3D LDA Data

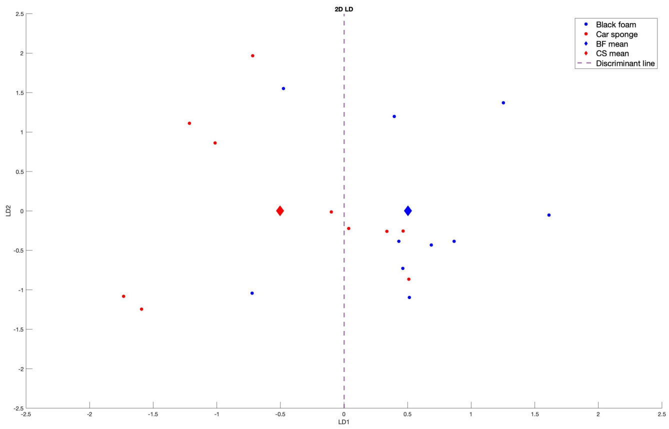

(b) 2D LDA Data

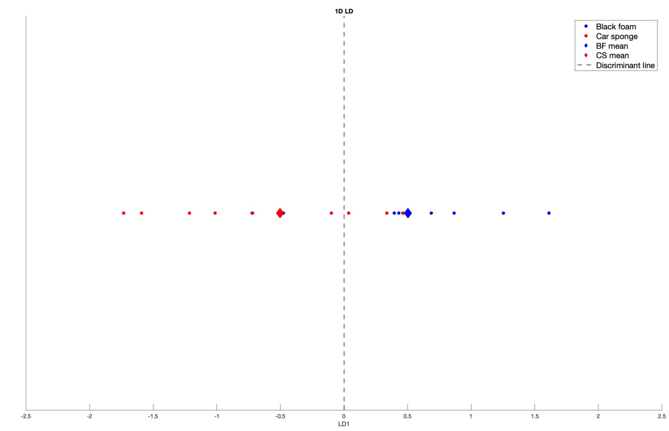

(c) 1D LDA Data

Figure C1.2: LDA Data for Black Foam and Car Sponge Objects for Reduced Dimensions

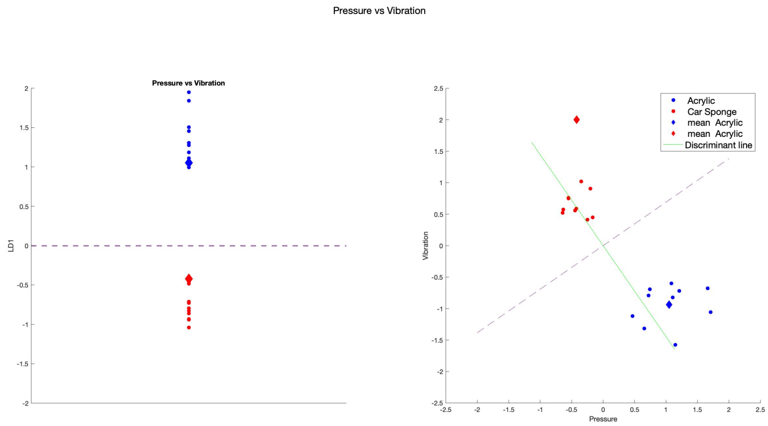

(a) Pressure vs Vibration

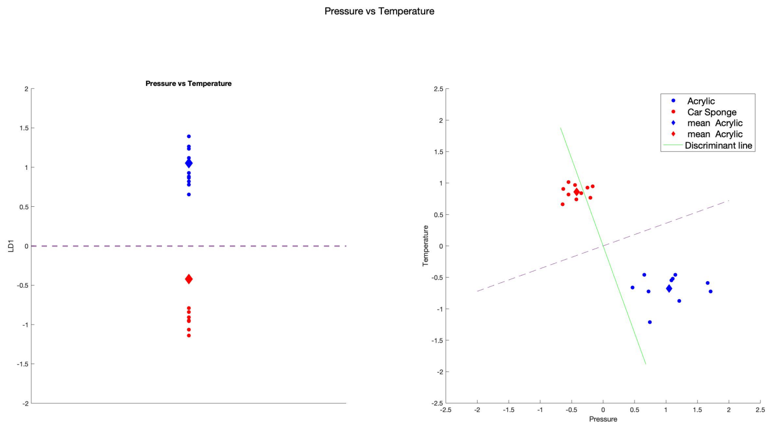

(b) Pressure vs Temperature

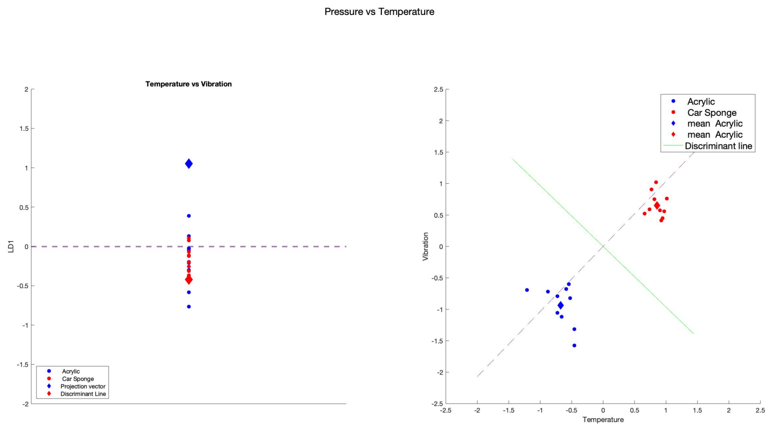

(c) Vibration vs Temperature

Figure C2.1: LDA Data for Acrylic and Car Sponge Objects

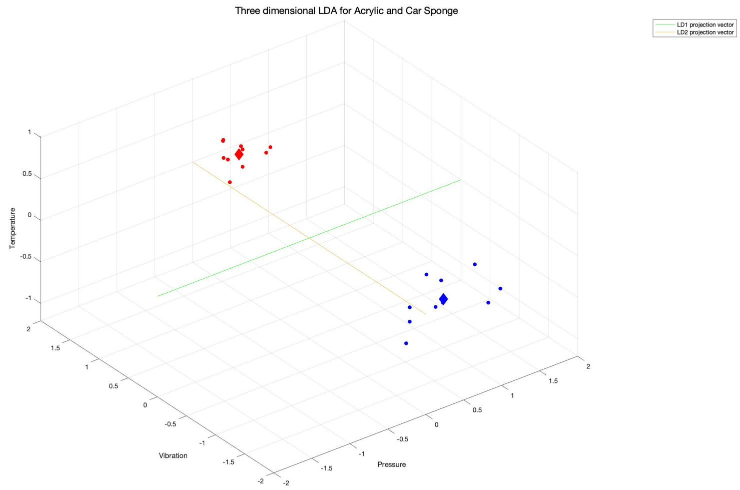

(a) 3D LDA Data

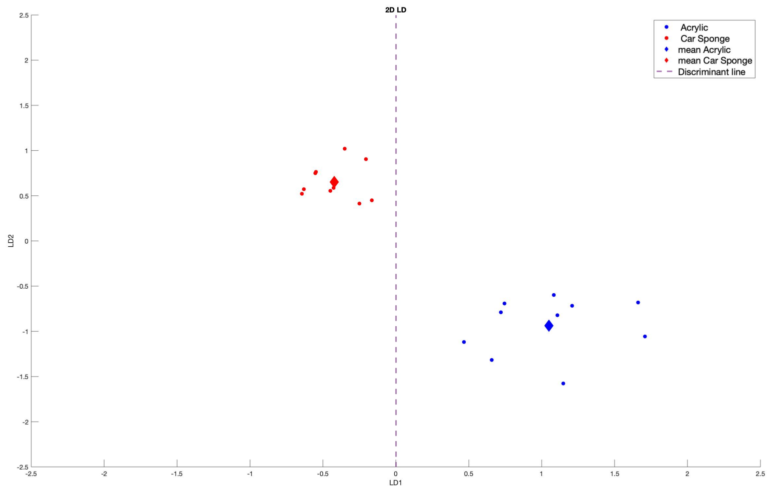

(b) 2D LDA Data

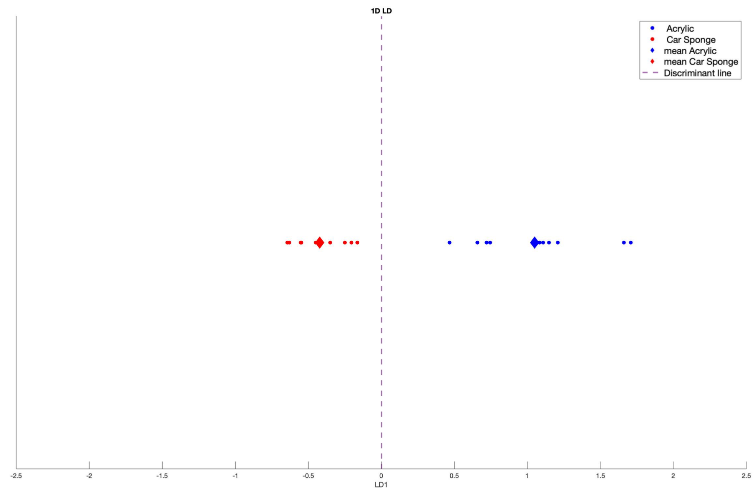

(c) 1D LDA Data

Figure C2.2: LDA Data for Acrylic and Car Sponge Objects for Reduced Dimensions

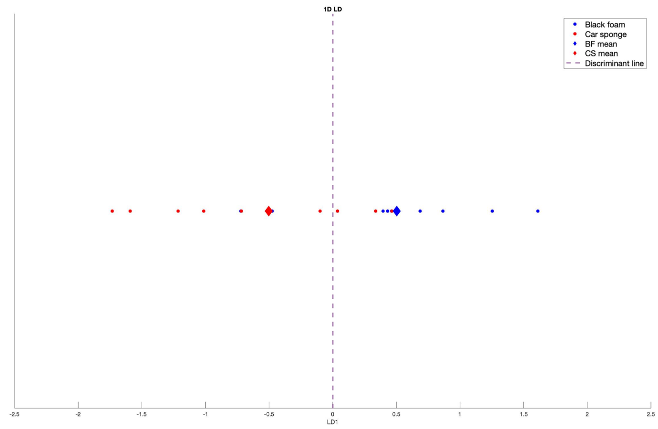

(a) Black Foam and Car Sponge

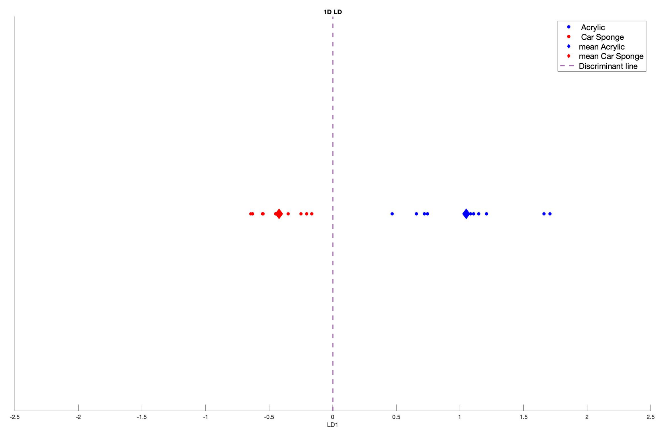

(b) Acrylic and Car Sponge Objects

Figure C1.2: 2D LDA Data for Comparison of Objects

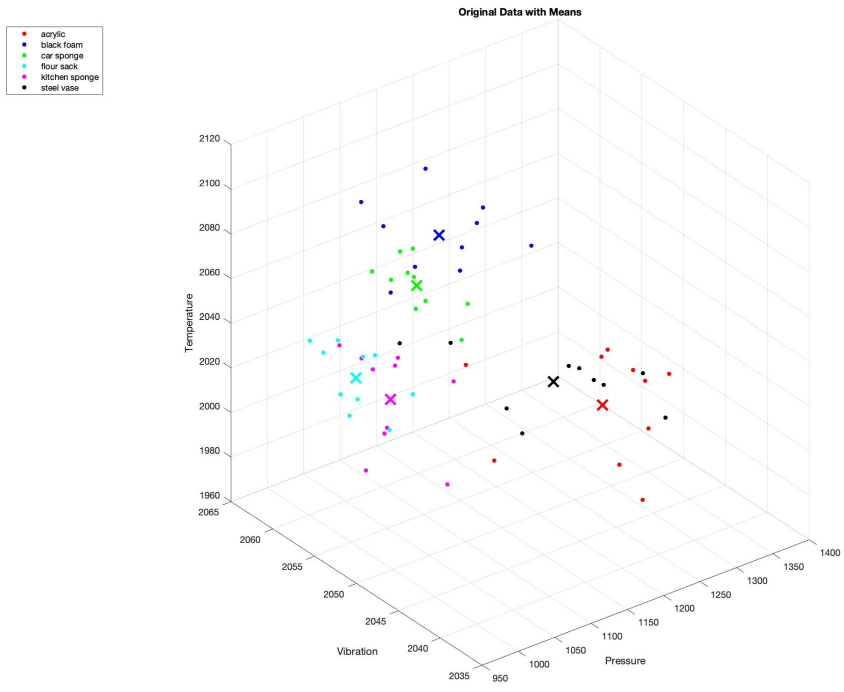

Figure D1.1: 3D Visualisation of PVT Data for Trial =9

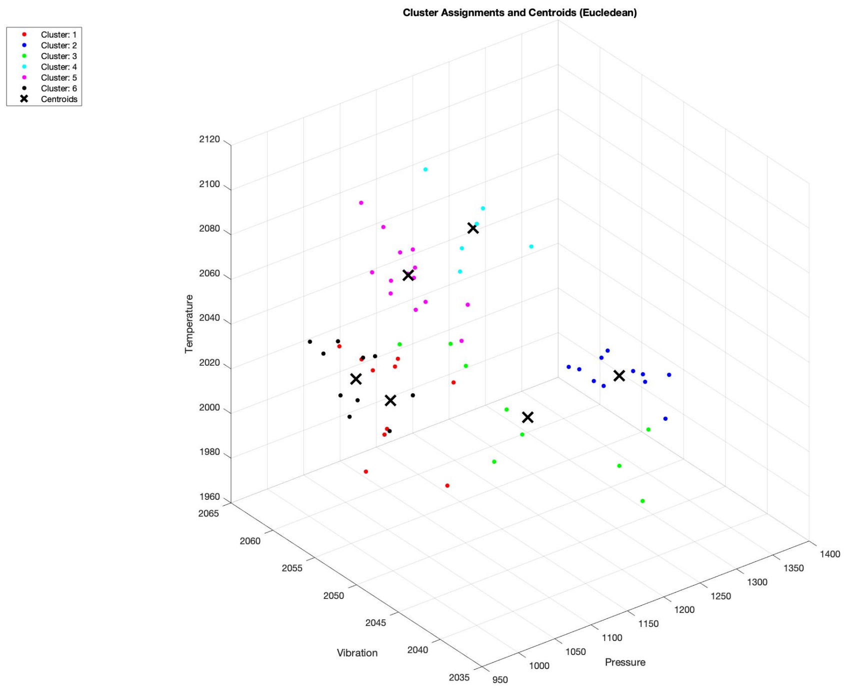

Figure D1.2: PVT Data: K-means Clustering Using Euclidean Distance Metric

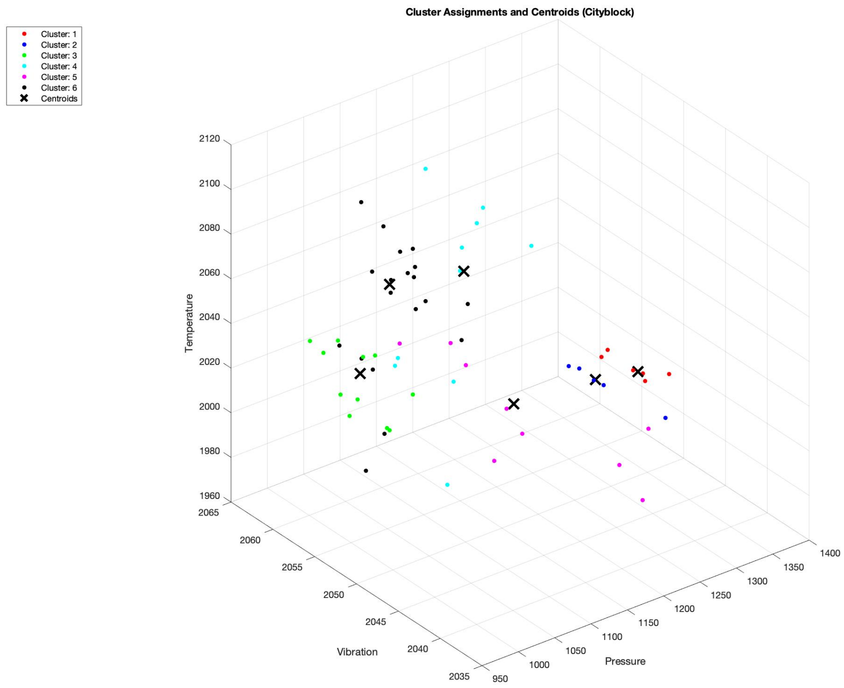

Figure D1.3: PVT Data K-means Clustering Using Citybook Distance Metric

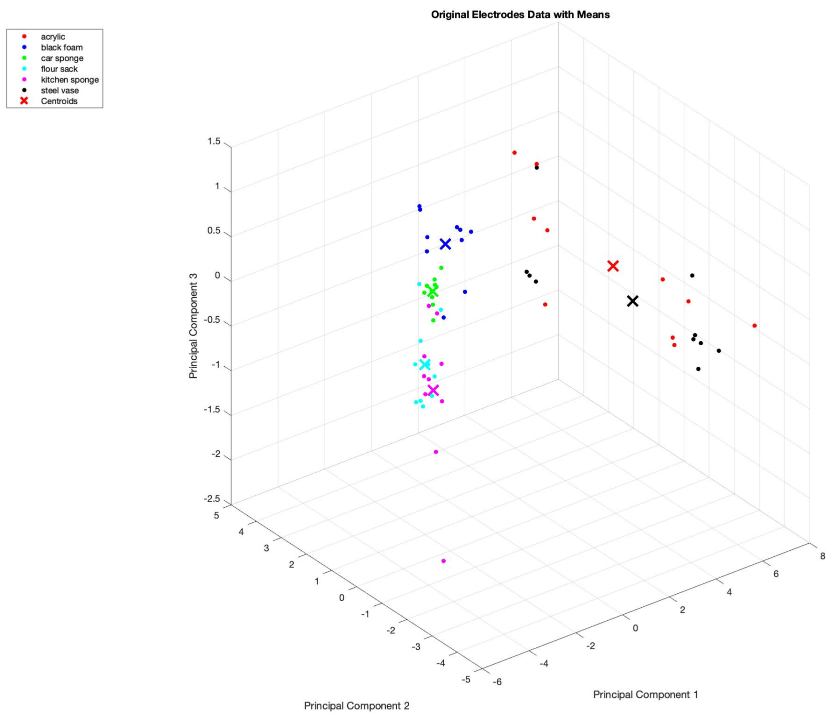

Figure D2.1: 3D Visualisation of PCA Electrode Data for Trial =9

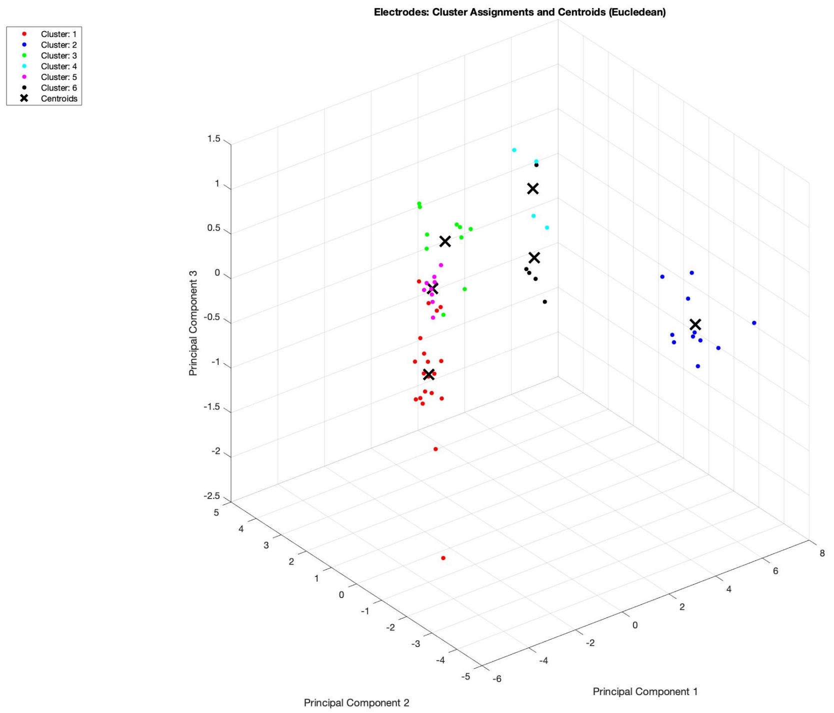

Figure D2.2: K-means Clustering Using Euclidean Distance Metric for PCA Electrode Data

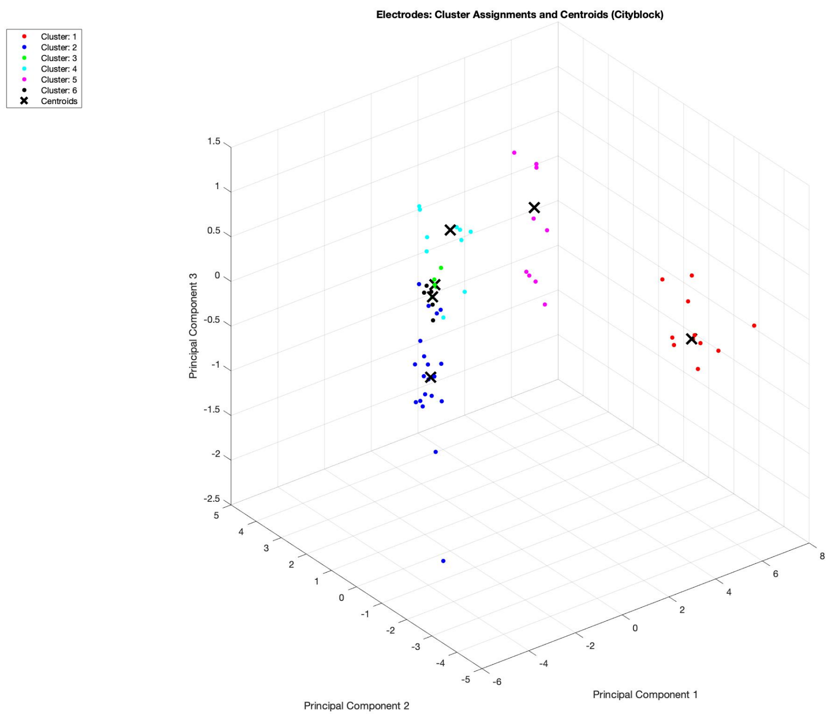

Figure D2.3: K-means Clustering Using Citybook Distance Metric for PCA Electrode Data

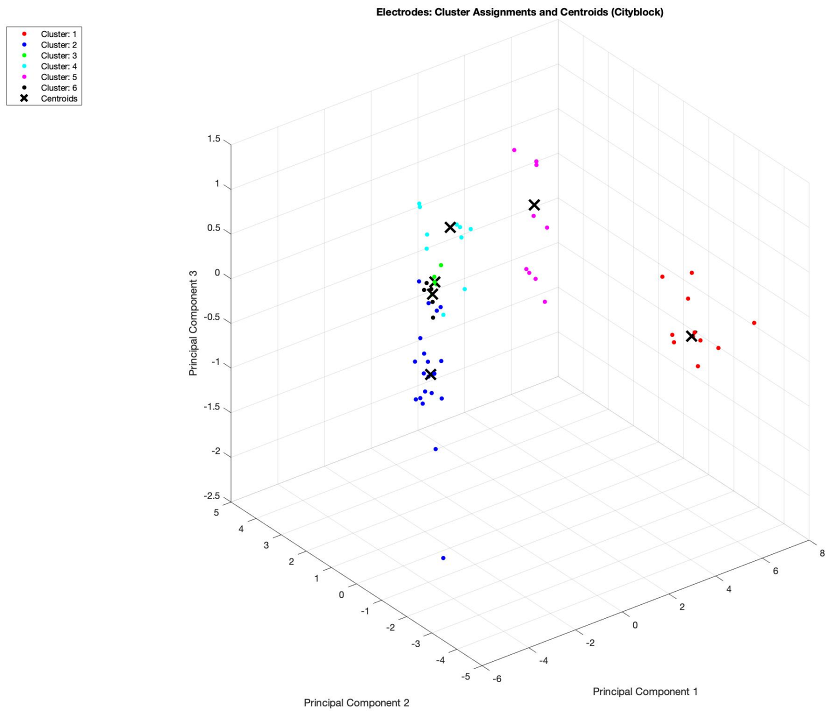

Figure D2.3:K-means Clustering Using Citybook Distance Metricfor for PCA Electrode Data

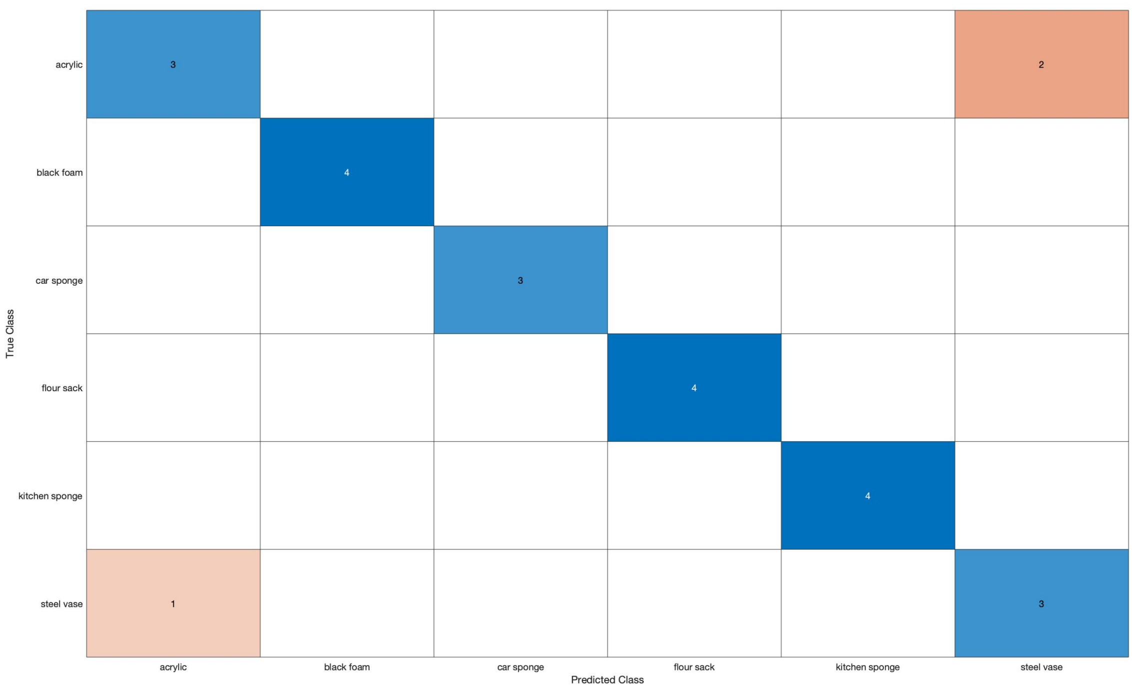

Figure D2.4:Confusion Matrix for PCA Electrode Data

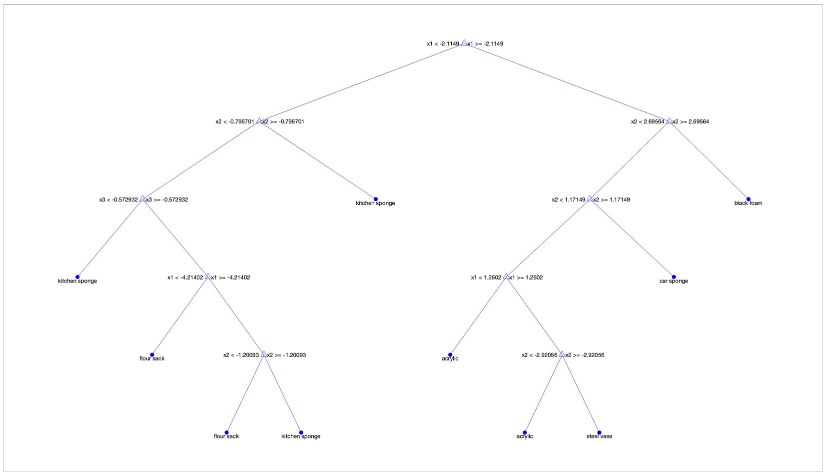

(a) Tree number:2

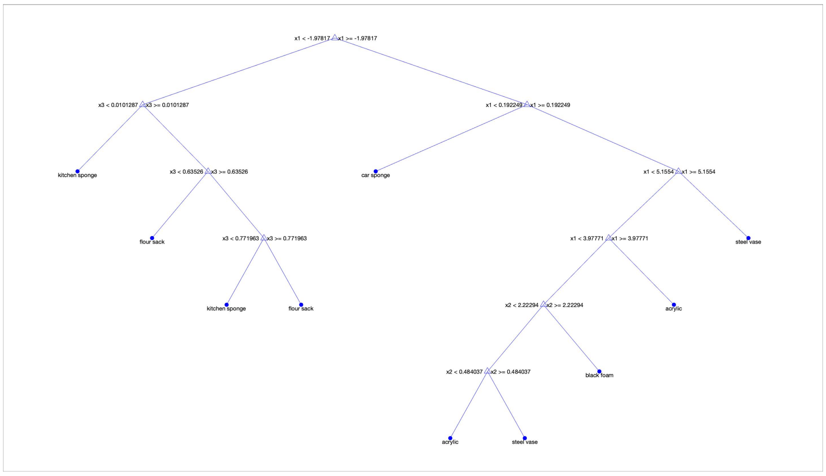

(b) Tree number:4

Figure D2.5: Decision Trees from Bagging for PCA Electrode Data

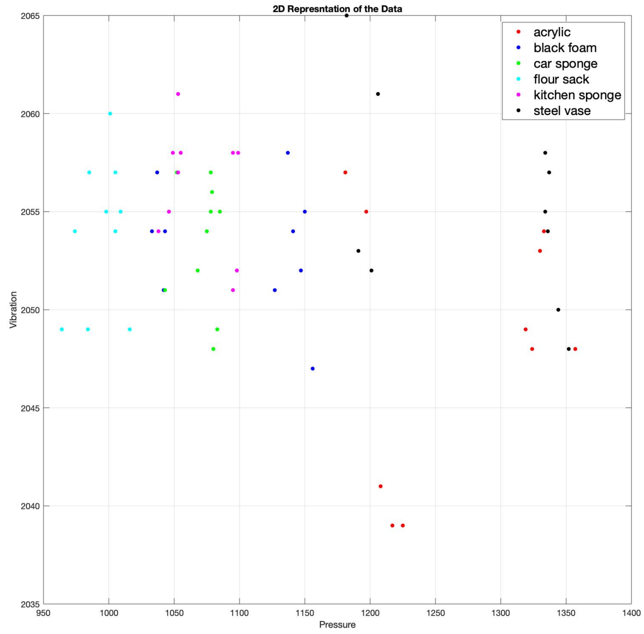

(a) 2D Data Representation Including Vibration Data

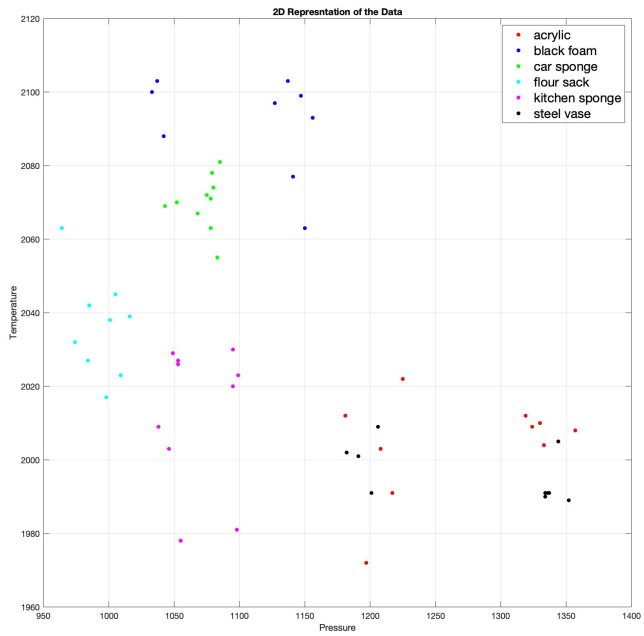

(b) 2D Data Representation Without Vibration Data

Figure E1.1: Vibration Data Effect in Object Separation